Absolute angle estimation by means of an IMU in a manipulator with electrohydraulic servo drives

Jarosław Gośliński*, **Piotr Owczarek****, **Dominik Rybarczyk****

*Faculty of Electrical Engineering, Poznań University of Technology, **Faculty of Mechanical Engineering and Management, Poznań University of Technology

Abstract: The problem of estimation of the manipulator's arm angle using the inertial measurement unit (IMU) is discussed. This unit was attached to the arm allowing identification of the arm's angle relatively to the global coordinate system. The manipulator was also equipped with two incremental encoders. Results of conducted experiments allowed to compare the pitch angle of the robot arm, estimated from the IMU and calculated from the encoder unit. In the study the influence of the IMU sensor position on the quality of estimates was verified. Parameters of the estimation algorithm have been also checked. Finally, the selected estimation algorithm was verified during the operation, where manipulator moved at various speeds and angles. Aim of this study was to test the angle estimation method using an IMU in the mechanical system with hydraulic drives.

Keywords: Kalman Filter, IMU, electrohydraulic manipulator, encoder

Measurement of the angle of the manipulator's arm is a task normally performed by the encoders, most often incremental. They allow to determine the tilt angle directly by counting the pulses in each robot's joint. This method enables accurate and robust closed-loop control. Encoder sensors, however, are expensive, generally more expensive than MEMS (Micro Electro-Mechanical Systems) sensors which tend to become even cheaper. The use of MEMS sensors would allow significant reduction of manufacturing costs of manipulators. In the literature attempts to introduce estimating systems for the position and orientation of the manipulator's joints based on accelerometers [1] and [2] can be seen ever more often.

Additionally, some works [3] introduce sophisticated methods that estimate the orientation and position of the manipulator's arm using accelerometers and gyroscopes. In this paper the authors attempt to introduce a simple system for estimating the tilt angle of the first arm of the robot using an IMU. For this purpose, hydraulic manipulator was used as a reference. It allows to compare the angle estimated form the IMU with the one calculated from the standard encoder. Authors decided to choose a hydraulic manipulator because of the possibility to set the position of the arm with motion of high dynamics and with disturbances characteristic for hydraulic systems.

1. The manipulator

Hydraulic manipulator, on which the research was conducted, is a system with three degrees of freedom, reminiscent of the construction of the lower limb without foot (fig. 1).

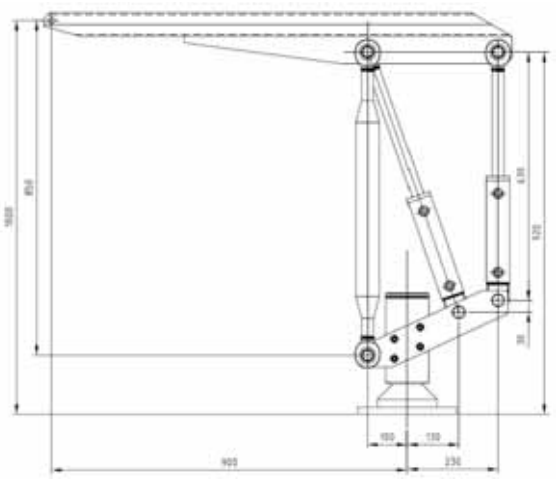

Fig. 1. Dimensions of the manipulator
Rys. 1. Wymiary manipulatora

It is a system equipped with three hydraulic pistons and servo-electric control. Master system imposes the robot's TCP (Tool Center Point) position by actuation of the hydraulic valve and simultaneous analysis of the position of the arm. Main feature of the above mentioned system is high dynamics of manipulator's movements. The manipulator provides a very good reference signal of changes in the position of the arm used in evaluation of the estimating algorithm.

2. Angle estimation

Angle estimation algorithms are based on MEMS sensors. The group of such sensors includes gyroscopes and accelerometers. These are inexpensive sensors, in which the fusion of information allows to obtain very good estimates of the measured physical quantity, assuming that setting, the estimation algorithm and the quality of the sensors are well suited to the application.

The problem with this type of system is an error which depends on the dynamics of the object on which the sensors are mounted. It is difficult to talk about the optimal settings for the estimator. Depending on the application in which the system works, suitable parameters should be set. A key issue is the algorithm for estimating a given quantity.

2.1. Estimation filters

Currently, different angle estimation algorithms are used in applications with IMU. Frequently Kalman filter is

exploited as the minimum variance estimator. It works in the following two stages:

1) Prediction of the estimated state, based on a process model or measurement.
2) Correction of the estimated state, based on a measurement.

This filter can be found in many varieties such as FKF (Fuzzy Tunned Kalman Filter) [4], Unscented Kalman Filter [5] or classic Kalman Filter.

Regardless of the type of the Kalman filter, there is always the problem of determination of filter settings. The filter defined as follows [6]:

1) Prediction phase

$$\underline{\hat{x}}_k^- = A_k \underline{\hat{x}}_{k-1}^- + B_k \underline{u}_{k-1} + w_{k+1}, \tag{1}$$

$$P_k^- = A_k P_{k-1} A_k^T + Q_k, \tag{2}$$

2) Correction phase

$$K_k = P_k^- C_k^T (C_k P_k^- C_k^T + R_k), \tag{3}$$

$$\underline{\hat{x}}_k = \underline{\hat{x}}_k^- + K_k(\underline{z}_k - (C_k \underline{\hat{x}}_k^- + v_k)), \tag{4}$$

$$P_k = (I - K_k C_k) P_k^-, \tag{5}$$

where process noise w_k is assumed to be white gaussian with parameters:

$$w_k \sim N(0, Q_k), \tag{6}$$

while measurement noise v_k, which is added to the output equation, has the following parameters:

$$v_k \sim N(0, R_k) \tag{7}$$

Settings to find for the presented filter are process noise variance Q_k and measurement noise variance R_k. Assumptions about the characteristics of the process noise and measurement noise strongly affect the results obtained during estimation of the state vector. The most common problem is the assumption of the additivity and the invariability of the process noise variance Q and the measurement noise variance R.

The first simplification is due to simplified noise model, which allows use of the Kalman filter in applications with complex structure. Further simplification of the Kalman filter, assuming constancy of variance is justified by the immutability of sensors. This means that the filter settings can be set as the variances of the sensors, without the consideration of the influence of physical effects on the overall estimation process. In the literature it very often comes down to the steady state Kalman filter [7]. Here authors decided to create the classic Kalman filter, for which the settings are adjusted after the experiment and the subsequent verification of estimation indicators.

The Kalman filter described by eqs. (1)–(5) can be used for a variety of linear systems for which it is possible to define matrices: A, B and C. Based on [8] a simple model of the estimator can be derived:

$$A_k = \begin{bmatrix} 1 & 0 & -dt \\ 0 & 0 & -1 \\ 0 & 0 & 1 \end{bmatrix}, \tag{8}$$

$$B_k = \begin{bmatrix} dt & 1 & 0 \end{bmatrix}^T, \tag{9}$$

$$C_k = \begin{bmatrix} 1 & 0 & 0 \end{bmatrix}^T, \tag{10}$$

where dt stands for the sample time of the integral used to calculate angle from angular velocity.

In addition, it is necessary to define the state vector $\underline{\hat{x}}_k$, input vector $\underline{u}_k$ and measurement vector $\underline{z}_k$:

$$\underline{\hat{x}}_k = \begin{bmatrix} \hat{\phi} & \dot{\hat{\phi}} & b \end{bmatrix}^T, \tag{11}$$

where $\hat{\phi}$ is the angle to be estimated, $\dot{\hat{\phi}}$ refers to angular velocity and b stands for the *bias* of the gyroscope.

The input vector has only one element and can be defined as:

$$\underline{u}_k = \dot{\phi} \tag{12}$$

The measurement vector, likewise the input vector, also has only one element:

$$\underline{z}_k = \phi_{\text{acc}} \tag{13}$$

In application, authors used 3-axial accelerometer and 3-axial gyroscope in one chassis (ADIS16405 from Analog Devices). Since the manipulator can be slightly moved in all three directions (X, Y and Z), angular velocity from the gyroscope and angle calculated from the accelerometer have to be transformed into the global coordinate system.

Starting from the gyroscope, it can be written that gyroscope measurement vector is equal to:

$$\underline{\Omega} = \begin{bmatrix} \omega_x \\ \omega_y \\ \omega_z \end{bmatrix} = \\ = \begin{bmatrix} \dot{\phi} \\ 0 \\ 0 \end{bmatrix} + C_X(\phi) \begin{bmatrix} 0 \\ \dot{\theta} \\ 0 \end{bmatrix} + C_X(\phi) C_Y(\theta) \begin{bmatrix} 0 \\ 0 \\ \dot{\psi} \end{bmatrix}, \tag{14}$$

which then may be written in a matrix form:

$$\underline{\Omega} = P_B^S \cdot \underline{\dot{\Theta}}, \tag{15}$$

where:

$$P_B^S = \begin{bmatrix} 1 & 0 & -\sin\theta \\ 0 & \cos\phi & \sin\phi\cos\theta \\ 0 & -\sin\phi & \cos\phi\cos\theta \end{bmatrix} \tag{16}$$

The next step is to calculate the inverse of the P_B^S matrix:

$$P_S^B = (P_B^S)^{-1} = \begin{bmatrix} 1 & \sin\phi\tan\theta & \cos\phi\tan\theta \\ 0 & \cos\phi & -\sin\phi \\ 0 & \frac{\sin\phi}{\cos\theta} & \frac{\cos\phi}{\cos\theta} \end{bmatrix} \tag{17}$$

Finally, having already the P_S^B matrix, which transforms raw angular velocities to the global coordinate system, Euler rates may be derived:

$$\underline{\dot{\Theta}} = \begin{bmatrix} \dot{\phi} \\ \dot{\theta} \\ \dot{\psi} \end{bmatrix} = P_S^B \cdot \underline{\Omega} \tag{18}$$

From eq. (18), term $\dot{\phi}$ is taken directly to the input vector $\underline{u}_k$ in eq. (12).

Similarly to Euler rates, also transformation for the accelerometer data must be done. In order to calculate Euler angles from the accelerations, one can use the general equations for the gravity vector in local coordinate system:

$$\underline{F}_g = \begin{bmatrix} a_x \\ a_y \\ a_z \end{bmatrix} = R_B^S(\underline{\Theta}) \cdot \begin{bmatrix} 0 \\ 0 \\ g \end{bmatrix} = \begin{bmatrix} -\sin\theta g \\ \sin\phi\cos\theta g \\ \cos\phi\cos\theta g \end{bmatrix}, \tag{19}$$

where $R_B^S(\underline{\Theta})$ is a transformation matrix (from global to local coordinate system):

$$R_B^S(\underline{\Theta}) = C_X(\phi) \cdot C_Y(\theta) \cdot C_Z(\psi) = \tag{20}$$

$$\begin{bmatrix} \mathrm{c}\theta\mathrm{c}\psi & \mathrm{c}\theta\mathrm{s}\psi & -\mathrm{s}\theta \\ \mathrm{s}\phi\mathrm{s}\theta\mathrm{c}\psi - \mathrm{c}\phi\mathrm{s}\psi & \mathrm{s}\phi\mathrm{s}\theta\mathrm{s}\psi + \mathrm{c}\phi\mathrm{c}\psi & \mathrm{s}\phi\mathrm{c}\theta \\ \mathrm{c}\phi\mathrm{s}\theta\mathrm{c}\psi + \mathrm{s}\phi\mathrm{s}\psi & \mathrm{c}\phi\mathrm{s}\theta\mathrm{s}\psi - \mathrm{s}\phi\mathrm{c}\psi & \mathrm{c}\phi\mathrm{c}\theta \end{bmatrix}, \tag{21}$$

Finally, based on $\underline{F}_g$, it can be written that:

$$\phi = \arctan(-\frac{a_y}{a_z}) \tag{22}$$

Angle from (22) goes to the vector $\underline{z}_k$. During the estimation process, state vector is updated twice per one measurment period dt. At first, prediction is available in $\underline{\hat{x}}_k^-$, after that, corrections are made directly on $\underline{\hat{x}}_k$.

3. The experiment

3.1. Description of the experiment

During the experiment, data was simultaneously collected from the encoder and the IMU system, with different Kalman Filter settings. For this purpose, the IMU sensor with the data processing system were mounted on the robot's arm (fig. 2).

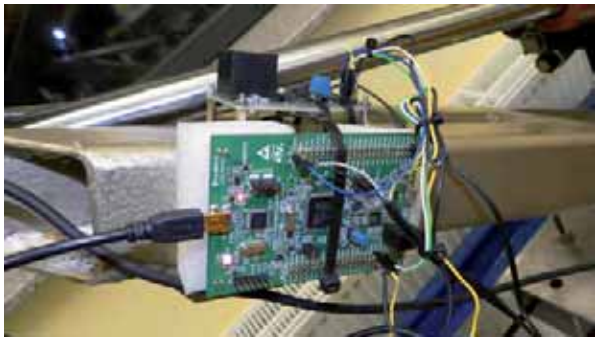

Fig. 2. IMU with STM processor during the experiment
Rys. 2. Jednostka IMU z procesorem STM podczas eksperymentu

The measurement cycle consists of few stages. At first, data is collected at the IMU and sent to the STM processor via SPI interface. Next, the data is transferred to a PC via RS232. On the PC side, C++ application, created in Microsoft Visual Studio (VS), receives the data and estimates the Euler angles. Additionaly, on PC, working Automation Studio (AS) receives data from the encoder and displays it in the main window of AS. AS also catches the estimated angle from VS via PVI (the tool for transferring the data). Finally, the angle obtained from the encoder (ϕ) and its estimate are saved to a file.

Overall communication process was presented in the fig. 3.

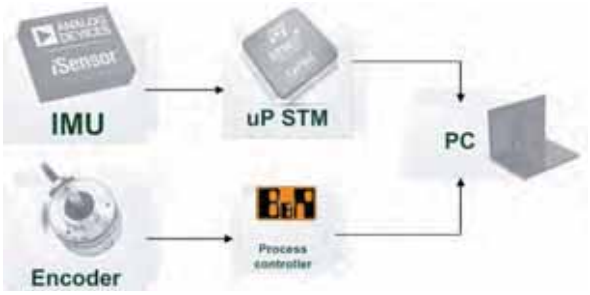

Fig. 3. Process of data gathering – a scheme
Rys. 3. Proces zbierania danych – schemat

3.2. Phases and process of the experiment

During the first phase of the experiment, the IMU was placed on the robot's arm at a distance of 55 cm from the joint, while in the second phase, it was mounted at a distance of 30 cm from the joint. The phases are illustrated in fig. 4.

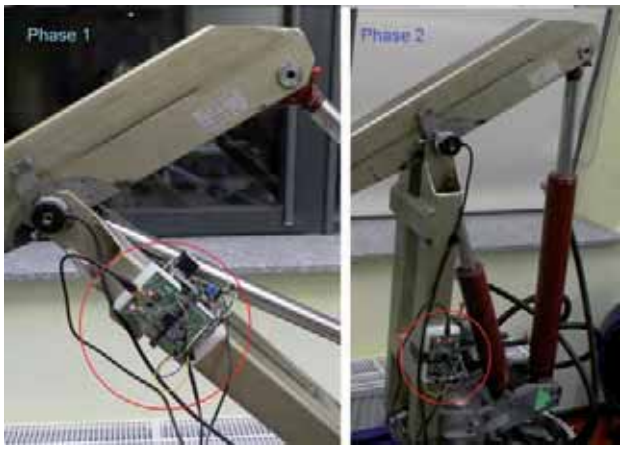

Fig. 4. Phases of the experiment
Rys. 4. Fazy eksperymentu

The experiment was carried out, taking into account only the first movement of the joint. This movement was executed with trapezoidal shape of the path.

4. Results

As previously stated, during the experiment, settings such as the Kalman filter process noise variance and the variance of the measurement noise (respectively Q_k and R_k) were subjected to change. In the first phase, when the sensor was located at the distance of 55 cm from the joint, the following responses from the estimator and the encoder were recorded:

- $Q_k = 0.01$, $R_k = 100$, fig. 5,
- $Q_k = 0.2$, $R_k = 10$, fig. 6,
- $Q_k = 4$, $R_k = 10$, fig. 7,
- $Q_k = 100$, $R_k = 10$, fig. 8,

As it can be seen, one may assess two parameters such as smoothness of the time-course and its fitness. There is a trade-off between these two features. At the time when the value of the noise process variance is increased, the filter reduces the confidence in the data from the gyro for the data from the accelerometer. In this case, significant

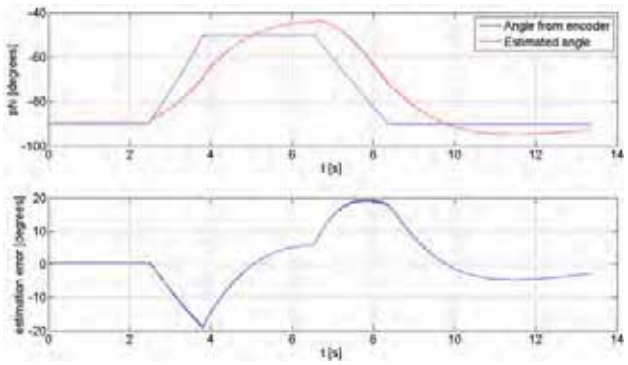

Fig. 5. Results for settings $Q_k = 0.01$, $R_k = 100$ (l = 55 cm)
Rys. 5. Wyniki dla nastaw $Q_k = 0{,}01$, $R_k = 100$ (l = 55 cm)

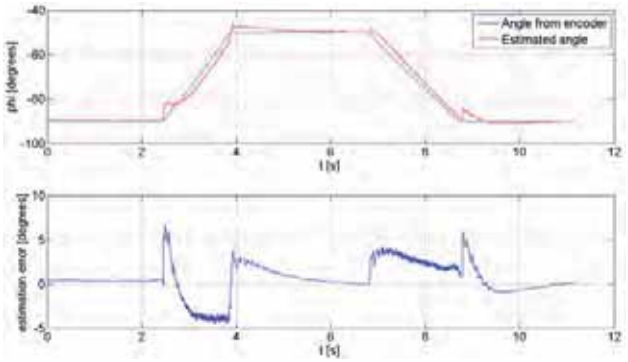

Fig. 6. Results for settings $Q_k = 0.2$, $R_k = 10$ (l = 55 cm)
Rys. 6. Wyniki dla nastaw $Q_k = 0{,}2$, $R_k = 10$ (l = 55 cm)

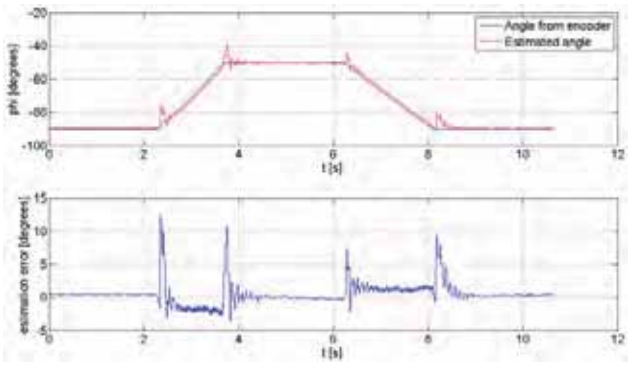

Fig. 7. Results for settings $Q_k = 4$, $R_k = 10$ (l = 55 cm)
Rys. 7. Wyniki dla nastaw $Q_k = 4$, $R_k = 10$ (l = 55 cm)

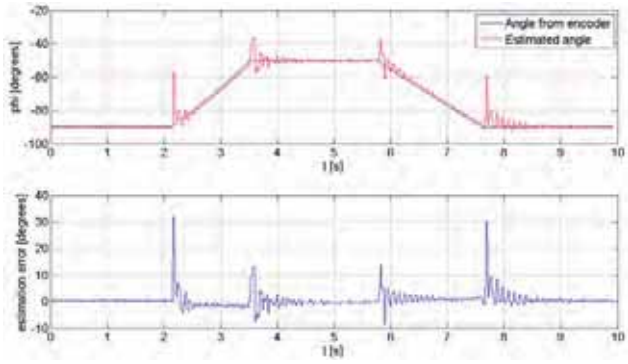

Fig. 8. Results for settings $Q_k = 100$, $R_k = 10$ (l = 55 cm)
Rys. 8. Wyniki dla nastaw $Q_k = 100$, $R_k = 10$ (l = 55 cm)

is only the ratio of these variances (i.e., Q_k and R_k). The authors also performed tests in the second phase, during which, the sensor was mounted 25 cm closer to the joint. For the example settings, the results were shown in the figs. 9, 10, 11 and 12.

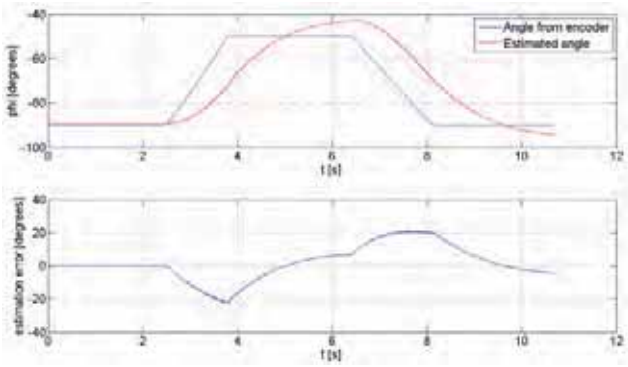

Fig. 9. Results for settings $Q_k = 0.01$, $R_k = 100$ (l = 30 cm)
Rys. 9. Wyniki dla nastaw $Q_k = 0{,}01$, $R_k = 100$ (l = 30 cm)

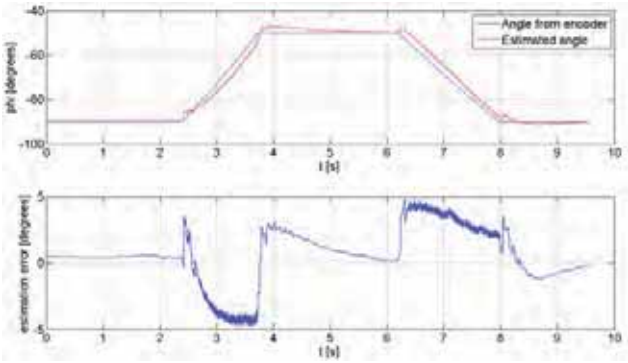

Fig. 10. Results for settings $Q_k = 0.2$, $R_k = 10$ (l = 30 cm)
Rys. 10. Wyniki dla nastaw $Q_k = 0{,}2$, $R_k = 10$ (l = 30 cm)

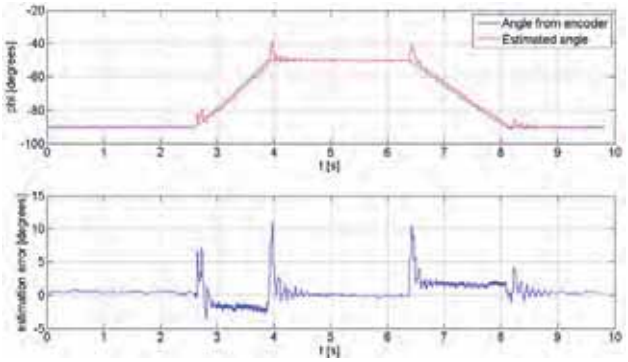

Fig. 11. Results for settings $Q_k = 4$, $R_k = 10$ (l = 30 cm)
Rys. 11. Wyniki dla nastaw $Q_k = 4$, $R_k = 10$ (l = 30 cm)

It can be seen that the shorter distance results in decrease of the maximum error of the estimator, which is clearly visible by comparing the plots in figs. 7 and 11.

In the next step, it was decided to compare all the results of collected data by introducing two quality estimation indicators. The first one is a ratio of the maximum value of the estimation error, which can be defined as:

$$e_{\max} = \max(e_k), \tag{23}$$

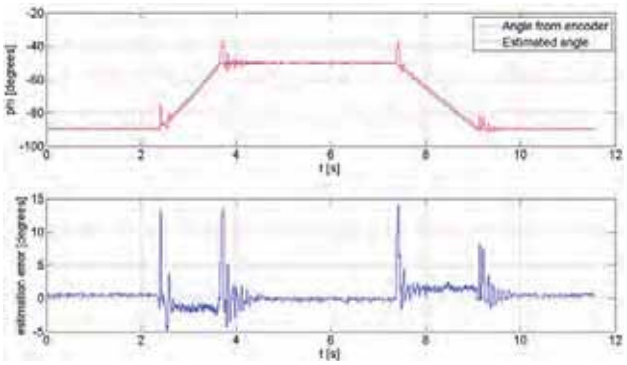

Fig. 12. Results for settings $Q_k = 100$, $R_k = 10$ (l = 30 cm)
Rys. 12. Wyniki dla nastaw $Q_k = 100$, $R_k = 10$ (l = 30 cm)

where e_k is an estimation error in a sample k calculated as a difference between ϕ estimated and calculated from the encoder:

$$e_k = \hat{\phi}_k - \phi_k \tag{24}$$

Another indicator is the sum of the square error, which can be expressed as follows:

$$e_{\text{sum}} = \sum_{k=0}^{k=n} e_k^2, \tag{25}$$

where n is the estimation horizon.

In tab. 1 all the indicators for the collected results were shown.

Tab. 1. Estimation quality indicators
Tab. 1. Wskaźniki jakości estymacji

No.	Q_k	R_k	$e_{\max}$ (*)	$e_{\max}$	e_{sum} (*)	e_{sum}
1.	0.01	100	19.63	22.76	997030	1175476
2.	0.1	100	12.24	12.53	277134	302106
3.	0.2	10	6.63	4.81	42812	44661
4.	0.5	10	8.35	6.01	33625	33012
5.	1	10	11.39	6.82	40446	21530
6.	4	10	12.39	10.76	33725	25247
7.	10	10	21.76	11.48	57806	25978
8.	100	10	32.12	14.16	94094	37130
* $l = 55$ cm						

In the results, regularity of growth of the integral while reducing the error variance Q_k or increasing the variance R_k can be seen. A similar situation is observed in the case of the maximum error, which is the smallest for the set $Q_k = 0.5$, $R_k = 10$, but it also strongly increases with the distance from the sensor to the joint. Regardless of the quality indicators, one will find that when comparing estimates, it is also necessary to assess the rate of changes, that is, the transmission of vibrations, which does not occur when the process noise variance Q_k is reduced to a certain level.

5. Summary and conclusions

In the carried out experiment, authors have focused on a comparison of the results from the estimator and the encoder. The comparison was made for different settings of the filter and for different locations of IMU mounting on the object of research. The results helped to determine that the best settings are near $Q_k = 1$ and $R_k = 10$. Additionally, it was confirmed that the closer to arm's joint the IMU is fixed, the better quality indicators can be achieved, particularly reducing the maximum error. The whole research was designed to verify operation of the Kalman Filter algorithm in estimation of the tilt angle in the applications with hydraulic drive.

The study confirmed possibilities of application of this type of sensory systems in manipulator with hydraulic drive. In the future, authors plan to enhance the system by introducing the low-pass filter for signals from the accelerometer along with automatic control of the Kalman Filter settings.

Acknowledgements

The work described in this paper was supported by the Ministry of Science and Higher Education of the Republic of Poland in the years 2009–2012, grant no. N502 260737.

References

1. Axelsson P., Norrlöf M., *Method to Estimate the Position and Orientation of a Triaxial Accelerometer Mounted to an Industrial Manipulator*, [in:] 10th International IFAC Symposium on Robot Control, Dubrovnik, Croatia, 2012.
2. Quigley M., Brewer R., Soundararaj S.P., Pradeep V., Le Q., Ng A.Y., *Low-cost Accelerometers for Robotic Manipulator Perception*, [in:] Proceedings of the Conference on Intelligent Robots and Systems (IROS), 2010, 6168–6174.
3. Roan P., Deshpande N., Wang Y., Pitzer B., *Manipulator State Estimation with Low Cost Accelerometers and Gyroscopes*, [in:] Proceedings of the Conference on Intelligent Robots and Systems (IROS), 2012.
4. Kang C.W., Park C.G., *Attitude Estimation with Accelerometers and Gyros Using Fuzzy Tuned Kalman Filter*, [in:] Proceedings of the European Control Conference, 2009, 3713–3718.
5. Zhang P., Gu J., Milios E.E., Huynh P., *Navigation with IMU/GPS/Digital Compass with Unscented Kalman Filter*, [in:] Proceedings of the IEEE International Conference on Mechatronics & Automation, 2005, 1497–1502.
6. Welch G., Bishop G., *An Introduction to the Kalman Filter*, TR-95-041, Department of Computer Science, University of North Carolina at Chapell Hill, 2002.
7. Li P., *Steady State Kalman Filter*, ME8281, M.E. University of Minnesota, 2008.
8. Kędzierski J., *Filtr Kalmana - zastosowania w prostych układach sensorycznych*, Koło Naukowe Robotyków KoNaR, update 2007, [www.konar.pwr.wroc.pl].

Estymacja kąta odchylenia za pomocą jednostki IMU w manipulatorze z serwonapędami elektrohydraulicznymi

Streszczenie: W artykule poruszono problem estymacji kąta wychylenia ramienia manipulatora przy użyciu inercyjnej jednostki pomiarowej (IMU). Jednostka została zamocowana na ramieniu manipulatora umożliwiając określenie odchylenia tego ramienia względem globalnego układu współrzędnych. Robot został również wyposażony w dwa enkodery inkrementalne. Wyniki pozwoliły na

porównanie estymaty kąta odchylenia ramienia robota obliczonej z jednostki IMU oraz enkodera. W pracy zweryfikowano wpływ położeniu czujnika IMU na jakość estymaty. Sprawdzeniu poddane zostały również nastawy algorytmu estymującego kąt odchylenia. Ostatecznie zweryfikowano działanie wybranego algorytmu estymującego kąt przy różnorodnych wymuszeniach ruchu manipulatora. Celem pracy było sprawdzenie metod estymujących kąt przy użyciu IMU w układach z napędem hydraulicznym.

Słowa kluczowe: filtr Kalmana, inercyjna jednostka pomiarowa, manipulator elektrohydrauliczny, enkoder

Jarosław Gośliński, MSc Eng

Received the MSc degree in control engineering and robotics from Poznan University of Technology (Poland) in 2011. He is currently a PhD student at the same university. His research interests include: signal filtering and processing, MEMS sensors, state observers, control of nonlinear and underactuated objects, swarm robotics and cyber-physical systems.

e-mail: jaroslaw.a.goslinski@doctorate.put.poznan.pl

Piotr Owczarek, MSc Eng

PhD student and assistant in Division of Mechatronics Devices in Poznan University of Technology. He graduated from electrical engineering, robotics and control engineering in 2011. His research interests include: modern methods of digital image processing, artificial intelligence methods, design of electronic and mechatronic devices, mobile robots and industrial controllers.

e-mail: piotr.owczarek@doctorate.put.poznan.pl

Dominik Rybarczyk, MSc Eng

Assistant in Division of Mechatronics Devices in Poznan University of Technology. Graduated from mechanical engineering at the same university in 2010. His research interests include: design of mechatronic devices, control of electrohydraulic servo drives, control of nonlinear objects and artificial intelligence methods.

e-mail: dominik.rybarczyk@put.poznan.pl